Hepatic fibrosis and angiogenesis after bile duct ligation are endogenously expressed vasohibin-1 independent

Yutaka Furutani [a], Yumi Shiozaki-Sato [a], Mitsuko Hara [a], Yasufumi Sato [b], Soichi Kojima [a, *]

[a] Micro-Signaling Regulation Technology Unit, RIKEN Center for Life Science Technologies, Saitama, 2-1 Hirosawa, Wako, Saitama 351-0198, Japan
[b] Department of Vascular Biology, Institute of Development, Aging and Cancer, Tohoku University, 4-1 Seiryo-machi, Aoba-ku, Sendai 980-8575, Japan

ARTICLE INFO

ABSTRACT

Liver fibrosis is linked to VEGF-induced angiogenesis. Overexpression of exogenous vasohibin-1, a feedback inhibitor of angiogenesis, has been reported to reduce liver fibrosis after bile duct ligation (BDL). To uncover the function of endogenous vasohibin-1, we performed BDL using vasohibin-1-deficient mice and analyzed liver fibrosis, injury, and angiogenesis. Liver fibrosis was induced by 14-days of BDL in both wild-type and vasohibin-1-deficient mice. The liver sections were stained with anti-CD31 to visualize endothelial cells and with Sirius red to observe fibrotic regions. Total RNAs were purified from the livers and expression of collagen I α1 mRNA was measured by quantitative PCR. Plasma ALT activity was determined to assess liver injury. Surprisingly, the same extents of increases were seen in anti-CD31 and Sirius red stainings, collagen I α1 mRNA expressions, hepatic hydroxyproline contents, and ALT activity after 14-days of BDL in both wild-type and vasohibin-1-deficient mice. There was unexpectedly no difference between these mice, suggesting that anti-fibrogenic and angiogenic activities of the endogenous vasohibin-1 might be masked in the normal liver at early stage of hepatic fibrosis in mice.

© 2015 Elsevier Inc. All rights reserved.

1. Introduction

Hepatic fibrosis progresses to cirrhosis and hepatic carcinoma mainly caused by infection of hepatitis virus, alcohol consumption, and non-alcoholic steatohepatitis (NASH) [1]. Up and down-regulation mechanisms of hepatic fibrosis are partly revealed with cytokines such as IL-1β, PDGF, TGF-β1, and TNFα for up-regulation and IFNα, IFNγ, IL-6, and IL-10 for down-regulation [2]. We have reported that daily injection of VEGF induces angiogenesis and hepatic fibrosis [3]. Angiogenesis links hepatic fibrogenesis, and many reports show that angiogenesis concomitantly progresses with fibrogenesis [4–11]. On the other hand, it is reported that resolution of hepatic fibrosis is associated by VEGF-regulated angiogenesis [12]. Thus, angiogenesis negatively and positively correlates hepatic fibrosis depending on degree of its fibrosis.

Vasohibin-1 (VASH1) is a negative feedback regulator of angiogenesis and expressed in endothelial cells under control of VEGF [13,14]. Coch et al. reported that overexpression of VASH1 reduces hepatic fibrogenesis, in vitro angiogenesis of HUVECs, and

mesenteric neovascularization in prevention trials [15]. In unilateral ureteral obstruction (UUO)-operated kidney, reduction of VASH1 expression level using VASH1 heterozygous knockout (ko) mice enhances renal fibrosis and inflammation [16]. In conclusion, VASH1 is implicated to be a negative regulator of angiogenesis and fibrosis.

However, endogenous VASH1 function in hepatic fibrosis remains unclear. We assume that hepatic fibrosis and angiogenesis are simultaneously enhanced in hepatic fibrosis model of VASH1-deficient mice. In this study, we tested this idea using a bile duct ligation (BDL) model of hepatic fibrosis and analyzed markers for fibrosis, liver injury, and angiogenesis. Analyses of these markers showed no significant difference between VASH1-deficient and wild-type mice.

2. Materials and methods

2.1. Bile duct ligation (BDL)

Eight to 9 weeks old wild-type (C57BL/6J; SLC, Japan) and VASH1-deficient mice [17] were subjected to BDL according Arias et al. [18]. After 2 weeks of ligation, the liver and blood were collected. These

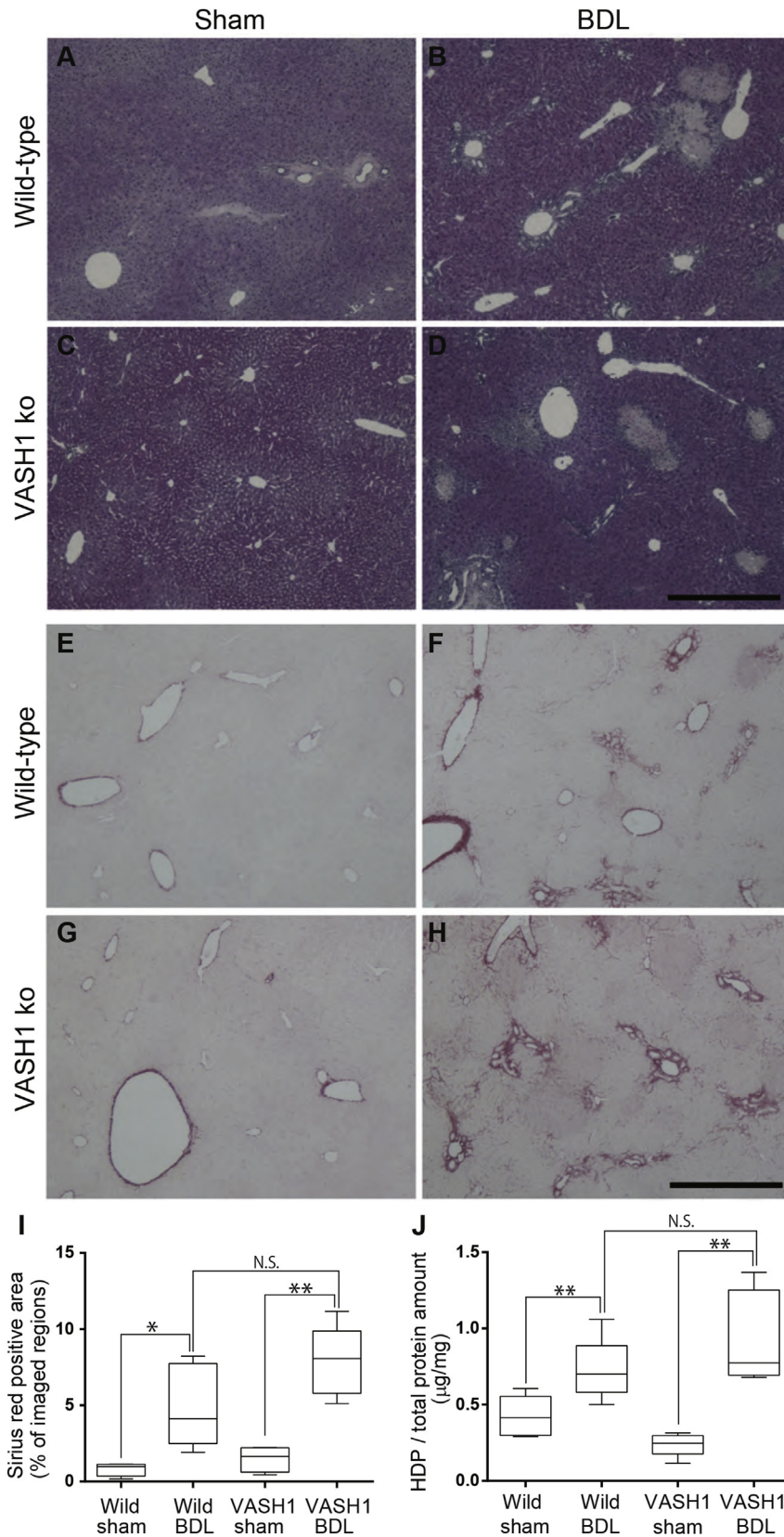* Corresponding author.
E-mail address: skojima@riken.jp (S. Kojima).

Fig. 1. Fibrotic regions analysis in BDL-operated VASH1-deficient and wild-type mice liver. (A–D) HE staining of sham-operated liver (A and C) and BDL-operated liver (B and D) in wild-type (A and B) and VASH1-deficient (C and D) mice (n = 4–6). (E–H) Sirius staining of sham-operated liver (E and G) and BDL-operated liver (F and H) in wild-type (E and F) and VASH1-deficient (G and H) mice (n = 4–6). Bars, 500 μm. (I) Box plots for liver fibrotic regions. These regions were calculated from percentage of Sirius red staining areas in the sham-operated wild-type (n = 4 mice) and VASH1-deficient (n = 4 mice) and BDL-operated wild-type (n = 5 mice) and VASH1-deficient (n = 6 mice) mice livers. Medians, middle lines; 75th and 25th quartiles, top and bottom lines, respectively; whiskers show range. *, $p < 0.05$; **, $p < 0.01$ (two-tailed t-test). (J) Hydroxyproline contents were divided with total protein amounts in the sham-operated wild-type (n = 6 mice) and VASH1-deficient (n = 5 mice) and BDL-operated wild-type (n = 6 mice) and VASH 1-deficient (n = 5 mice) mice livers. **, $p < 0.01$ (two-tailed t-test).

animal experiments were approved by RIKEN Institutional Animal Use and Care Administrative Advisory Committee.

2.2. Hematoxylin and Eosin (HE) and Sirius red staining

Both BDL-operated and sham-operated livers were fixed in 4% PFA/PBS overnight. Blocks of the liver were embedded in paraffin and cut into 5 μm sections. The sections were deparaffinized and stained with HE or 0.1% picro-Sirius red solution, and then mounted on malinol. HE staining and Sirius red staining were imaged by Nikon ECLIPSE 55i microscopy using Plan Fluor 4x/0.13 objective (Nikon). After trimming of edge regions within the liver sections, Sirius red-stained regions and areas of liver sections in partly overlapped 2-4 images depending on the section size were measured by WinROOF image analysis software (Nikon).

2.3. Measurement of hydroxyproline content

Hepatic hydroxyproline (HDP) contents were measured as described previously [3], and expressed in μg/mg of sample proteins.

2.4. ALT assay

Blood samples were blocked its coagulation using 5 mM EDTA. After 10 min of centrifugation at $3000 \times g$, supernatants were collected as plasma. Plasma ALT activity was measured using ALT assay kit (BioVision), according to manufacturer's instruction.

2.5. Immunofluorescent staining of CD31

Liver blocks were snap frozen in O.C.T. compound and sectioned at 20 μm thickness. The sections were fixed with methanol for 30 min at −20 °C, blocked with 10% goat serum in PBS, incubated with anti-CD31 (1/100: BD) overnight at room temperature. The first antibody and nucleus were visualized with Alexa488-conjugated goat anti-rat IgG (1/500: Lifetechnologies) and Hoechst 33258 (1 μg/ml), respectively. The sections were embedded in Fluoromount (Diagnostic BioSystem). Fluorescent images were acquired by a Zeiss LSM700 laser scanning confocal microscopy using 10x objective (Zeiss Plan-Apchromat, 10x/0.45). Fluorescent intensities of Alexa488 were measured and averaged from 3 imaged regions around sinusoidal vein within the liver section. The lowest averaged intensity was subtracted from the other averaged intensities, and these values were calculated and shown as box-and-whisker plots.

2.6. Quantitative PCR of collagen I α1 and VASH1

Total RNAs were purified from the BDL- or sham-operated livers using an RNeasy mini kit (Qiagen). The 500 ng each of total RNAs were reverse-transcribed using PrimeScript RT Master Mix Perfect (Takara). cDNAs and specific primer pairs were mixed with SYBR Premix Ex Taq II (Takara), and then quantitative PCR was performed using Light Cycler 96 system (Roche). The specific primer pairs used in this experiments were collagen I α1 (Fr, 5′-TGTTCAGCTTTGTG-GACCTC-3′: Rv, 5′-TCAAGCATACCTCGGGTTTC-3′), VASH1 (Fr, 5′-CATCAGGGAGCTGCAGTACA-3′: Rv, 5′-TTGATTGGCAGAGCCT CTTT-3′), and GAPDH (Fr, 5′ AACTTTGGCATTGTGGAAGG-3′: Rv, 5′-GGATGC AGGGATGATGTTCT-3′).

3. Results

VASH1 is known as a suppressor of angiogenesis. Furthermore, overexpression of VASH 1 in the liver suppresses liver fibrosis after BDL. We reported that liver fibrosis and angiogenesis were

simultaneously enhanced upon daily injection of VEGF to mice [3]. Hence, we thought that liver fibrosis and angiogenesis were further enhanced in VASH 1-deficient mice after BDL compared to wild-type mice.

3.1. Liver fibrosis

We performed BDL using VASH 1-deficient and wild-type mice, and then the liver and blood were collected and analyzed for Sirius red- and CD31-stainings, collagen I α1 mRNA expressions, hydroxyproline measurements, and ALT assay after 14 days of ligation. Paraffin embedded liver sections were stained with Hematoxylin and Eosin (HE) and picro/Sirius red. Results are shown in Fig. 1A–D and E–H. Percentage of Sirius red-staining areas in the liver sections were calculated in Fig. 1I. Sirius red positive fibrotic area increased after BDL in both mice. Ratio of fibrotic areas appeared to increase in VASH1-deficient mice compared to wild-type mice (Fig. 1F and H), but their differences were not statistically significant (Fig. I). In addition, protein expression levels of accumulated collagen measured by HDP amounts were also enhanced after BDL, but were not significantly different between wild-type and VASH 1-deficient mice (Fig. 1J). Levels of mRNA expression of collagen I α1, analyzed by quantitative PCR, were also not significantly different between wild-type and VASH1-deficient mice (Fig. 2A). We confirmed enhancement of VASH1 expression in the wild-type mice livers after 14-days of BDL (Fig. 2B). Liver fibrosis was induced after BDL, but not further up-regulated in BDL-operated VASH 1-deficient mice compared to wild-type mice.

3.2. Liver injury

As liver injury is accompanied by liver fibrosis, we measured plasma ALT assay. Plasma ALT level were significantly increased after BDL in both wild type and VASH1-deficient mice, but not significantly different between these mice (Fig. 3). Thus, liver injury was not further enhanced in the BDL-operated VASH1 ko mice.

3.3. Angiogenesis

To reveal relation between angiogenesis and liver fibrosis, an endothelial cell marker CD31 was stained in the BDL-and sham-operated wild and VASH1-deficient mice liver sections (Fig. 4A–D). CD31-staining intensity was significantly increased after BDL in both mice liver sections, but not different between BDL-operated
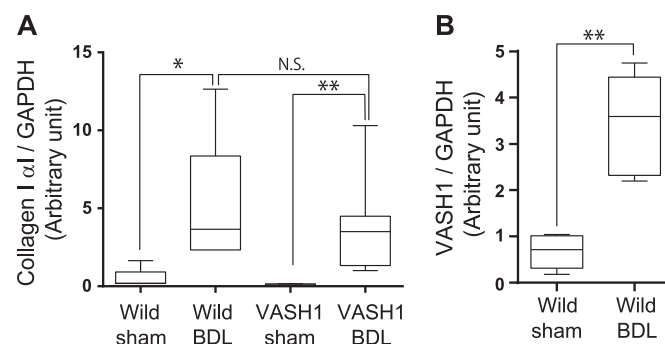

Fig. 2. Liver fibrotic marker (Collagen I α1) and angiogenesis suppressor (VASH1) mRNA expression in sham- and BDL-operated mice. Box plots for expression collagen I α1 (A) and VASH1 (B) mRNAs were shown. Quantitative PCRs were performed using cDNAs prepared from the sham-operated wild-type (n = 5 mice) and VASH1-deficient (n = 8 mice) and BDL-operated wild-type (n = 5 mice) and VASH1-deficient (n = 8 mice) mice livers. The expression levels were normalized by GAPDH contents. Medians, middle lines; 75th and 25th quartiles, top and bottom lines, respectively; whiskers show range. *, p < 0.05; **, p < 0.01 (two-tailed t-test).
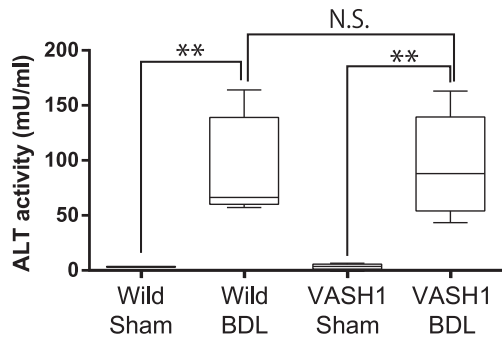
Fig. 3. Liver injuries analyzed by plasma ALT level. Box plots for plasma ALT activity. ALT assay was performed in the sham-operated wild-type (n = 4 mice) and VASH1-deficient (n = 6 mice) and BDL-operated wild-type (n = 5 mice) and VASH1-deficient (n = 8 mice) mice plasma. Medians, middle lines; 75th and 25th quartiles, top and bottom lines, respectively; whiskers show range. **, p < 0.01 (two-tailed *t*-test).

these mice (Fig. 4E). Therefore, although CD31-staining and liver fibrosis were concomitantly increased after BDL as previously reported, CD31-staining and liver fibrosis were not further enhanced in the BDL-operated VASH1-deficient mice livers.

4. Discussion

In this study, we made a BDL fibrosis model of the liver in VASH1-deficient mice, and analyzed hepatic fibrosis, injury, and angiogenesis to uncover a role of endogenous VASH1. As Coch et al. reported that adenoviral overexpression of VASH1 in the rat liver reduced hepatic fibrosis after BDL compared to control adenoviral infection [15], we speculated exacerbation of hepatic fibrosis in VASH1-deficient mice. However, VASH1 ablation did not influence hepatic fibrosis in our study; None of liver fibrosis, injury, and angiogenesis was not significantly different comparing to those in wild-type mice. VASH1 is originally cloned as a negative feedback regulator of angiogenesis and its expression is induced by VEGF [14]. Endogenous VASH1 expression in the mouse livers was increased (Fig. 2B) along with increased VEGF expression after BDL-operation [15]. However, as basal VASH1 expression levels were quite low in the liver comparing to those in the kidney [14], even after upregulation due to BDL, VASH1 expression levels in the liver might not be enough to reduce angiogenesis and hepatic fibrosis at early stage of hepatic fibrosis comparing to exogenously administrated levels [14,15]. Namely, adenoviral overexpression of VASH1 achieved high levels enough to reduce hepatic fibrosis, while enhanced levels of VASH1 during 2 weeks of BDL might not be effective to reduce hepatic fibrosis. In contrast to the current results in the liver, renal fibrosis in VASH1-heterogenic mice is exacerbated compared to wild-type mice [16]. Estimated from the result of quantitative PCR of VASH1 mRNA in sham- and BDL-operated mice liver (Fig. 2B) and data in the previous paper of northern blot analysis of VASH1 mRNA expression in the liver and kidney [14], VASH1 expression levels after 2 weeks of BDL appeared comparable to endogenous VASH1 expression levels in the kidney. Thus, an activity of VASH1 could be masked in the liver but unmasked in the kidney. If so, we need to determine molecular mechanism of the masking the activity of endogenous VASH1 in the liver.
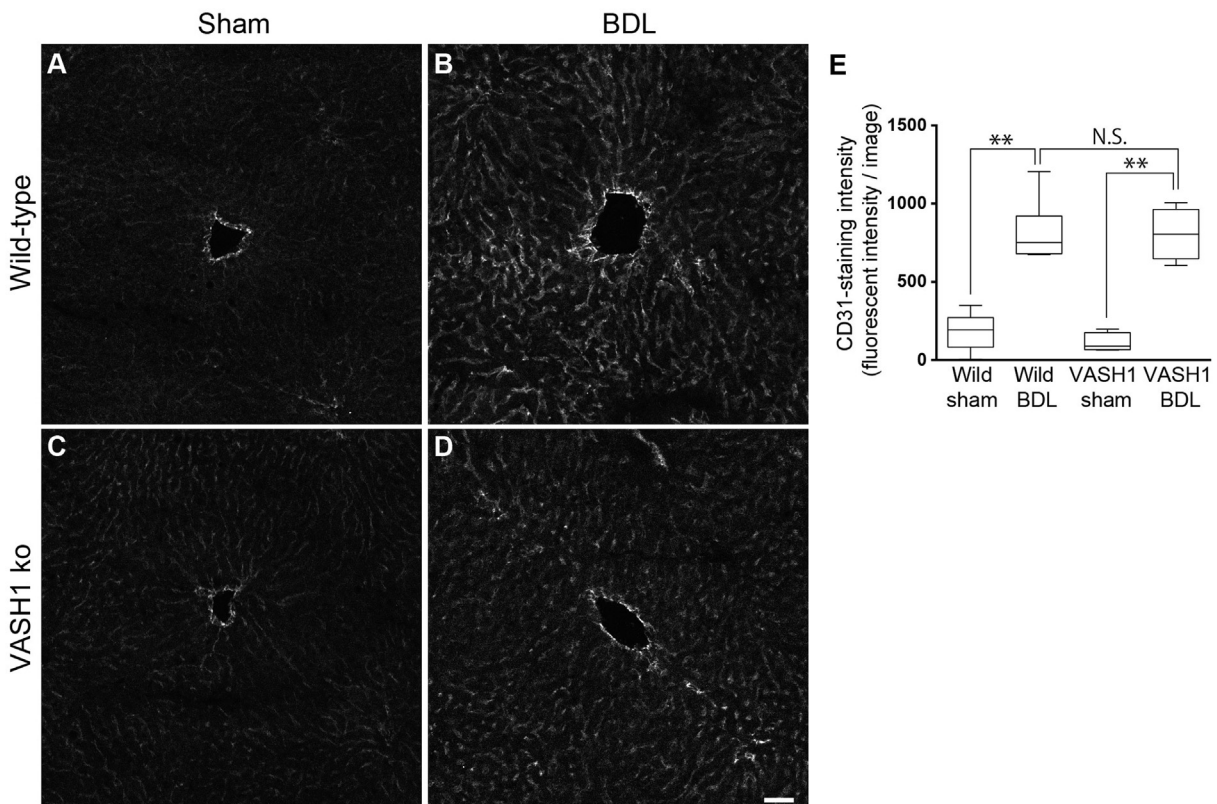

Fig. 4. Angiogenesis analysis in the BDL-operated VASH1-deficient and wild-type mice liver. (A–D) CD31 (endothelial cells marker)-staining of sham-operated liver (A and C) and BDL-operated liver (B and D) in wild-type (A and B) and VASH1-deficient (C and D) mice. Bar, 50 μm. (E) Box plots for CD31 staining intensities. CD31 staining intensities were calculated and averaged from randomly selected 3 images each for the sham-operated wild-type (n = 5 mice), sham-operated VASH1-deficient (n = 4 mice), BDL-operated wild-type (n = 6 mice), and BDL-operated VASH1-deficient (n = 4 mice) mice liver sections. The lowest averaged intensity was subtracted from the other averaged intensities, and these values were shown as box plots. Medians, middle lines; 75th and 25th quartiles, top and bottom lines, respectively; whiskers show range. **, p < 0.01 (two-tailed *t*-test).

Angiogenesis positively and negatively regulates hepatic fibrosis under control of VEGF. We reported that daily injection of VEGF into mice simultaneously promotes angiogenesis and fibrogenesis via supplying latent TGF-β in the livers at the early stage of fibrosis [3]. In contrast, Kantari-Mimoum et al. reported that myeloid cell-derived VEGF promoted angiogenesis and resolution of liver fibrosis via activation of matrix metalloproteases (MMPs) in the fibrotic region at late stage of fibrosis [12]. It is intriguing to measure VASH1 levels in these models.

Both anti-angiogenic and fibrogenic activities of VASH1 might be masked at lower expression levels in the liver especially at early stage of hepatic fibrosis. It might be possible that endogenous VASH1 will function at late stage of hepatic fibrosis where VASH1 expression levels may be relatively higher than those at early stage of hepatic fibrosis. In conclusion, we demonstrated that VASH1 is upregulated during BDL, but both anti-angiogenesis and anti-fibrogenesis effects are dispensable at early stage of hepatic fibrosis.

Conflict of interest

None.

Acknowledgments

Transparency document

Transparency document related to this article can be found online at http://dx.doi.org/10.1016/j.bbrc.2015.05.074.

References

[1] J.P. Iredale, Models of liver fibrosis: exploring the dynamic nature of inflammation and repair in a solid organ, J. Clin. Invest. 117 (2007) 539–548.

[2] K. Wallace, A.D. Burt, M.C. Wright, Liver fibrosis, Biochem. J. 411 (2008) 1–18.

[3] K. Sakata, S. Eda, E.S. Lee, M. Hara, M. Imoto, S. Kojima, Neovessel formation promotes liver fibrosis via providing latent transforming growth factor-beta, Biochem. Biophys. Res. Commun. 443 (2014) 950–956.

[4] C. Corpechot, V. Barbu, D. Wendum, N. Kinnman, C. Rey, R. Poupon, C. Housset, O. Rosmorduc, Hypoxia-induced VEGF and collagen I expressions are associated with angiogenesis and fibrogenesis in experimental cirrhosis, Hepatology 35 (2002) 1010–1021.

[5] K. Jagavelu, C. Routray, U. Shergill, S.P. O'Hara, W. Faubion, V.H. Shah, Endothelial cell toll-like receptor 4 regulates fibrosis-associated angiogenesis in the liver, Hepatology 52 (2010) 590–601.

[6] C. Paternostro, E. David, E. Novo, M. Parola, Hypoxia, angiogenesis and liver fibrogenesis in the progression of chronic liver diseases, World J. Gastroenterol. 16 (2010) 281–288.

[7] K. Taura, S. De Minicis, E. Seki, E. Hatano, K. Iwaisako, C.H. Osterreicher, Y. Kodama, K. Miura, I. Ikai, S. Uemoto, D.A. Brenner, Hepatic stellate cells secrete angiopoietin 1 that induces angiogenesis in liver fibrosis, Gastroenterology 135 (2008) 1729–1738.

[8] L. Yang, S. Yue, L. Yang, X. Liu, Z. Han, Y. Zhang, L. Li, Sphingosine kinase/sphingosine 1-phosphate (S1P)/S1P receptor axis is involved in liver fibrosis-associated angiogenesis, J. Hepatol. 59 (2013) 114–123.

[9] C. Stockmann, Y. Kerdiles, M. Nomaksteinsky, A. Weidemann, N. Takeda, A. Doedens, A.X. Torres-Collado, L. Iruela-Arispe, V. Nizet, R.S. Johnson, Loss of myeloid cell-derived vascular endothelial growth factor accelerates fibrosis, Proc. Natl. Acad. Sci. U. S. A. 107 (2010) 4329–4334.

[10] H. Sahin, E. Borkham-Kamphorst, C. Kuppe, M.M. Zaldivar, C. Grouls, M. Alsamman, A. Nellen, P. Schmitz, D. Heinrichs, M.L. Berres, D. Doleschel, D. Scholten, R. Weiskirchen, M.J. Moeller, F. Kiessling, C. Trautwein, H.E. Wasmuth, Chemokine Cxcl9 attenuates liver fibrosis-associated angiogenesis in mice, Hepatology 55 (2012) 1610–1619.

[11] D. Thabut, C. Routray, G. Lomberk, U. Shergill, K. Glaser, R. Huebert, L. Patel, T. Masyuk, B. Blechacz, A. Vercnocke, E. Ritman, R. Ehman, R. Urrutia, V. Shah, Complementary vascular and matrix regulatory pathways underlie the beneficial mechanism of action of sorafenib in liver fibrosis, Hepatology 54 (2011) 573–585.

[12] C. Kantari-Mimoun, M. Castells, R. Klose, A.K. Meinecke, U.J. Lemberger, P.E. Rautou, H. Pinot-Roussel, C. Badoual, K. Schrodter, C.H. Osterreicher, J. Fandrey, C. Stockmann, Resolution of liver fibrosis requires myeloid cell-driven sinusoidal angiogenesis, Hepatology 61 (2015) 2042–2055.

[13] Y. Sato, The vasohibin family: a novel family for angiogenesis regulation, J. Biochem. 153 (2013) 5–11.

[14] K. Watanabe, Y. Hasegawa, H. Yamashita, K. Shimizu, Y. Ding, M. Abe, H. Ohta, K. Imagawa, K. Hojo, H. Maki, H. Sonoda, Y. Sato, Vasohibin as an endothelium-derived negative feedback regulator of angiogenesis, J. Clin. Invest. 114 (2004) 898–907.

[15] L. Coch, M. Mejias, A. Berzigotti, E. Garcia-Pras, J. Gallego, J. Bosch, R. Mendez, M. Fernandez, Disruption of negative feedback loop between vasohibin-1 and vascular endothelial growth factor decreases portal pressure, angiogenesis, and fibrosis in cirrhotic rats, Hepatology 60 (2014) 633–647.

[16] H. Watatani, Y. Maeshima, N. Hinamoto, H. Yamasaki, H. Ujike, K. Tanabe, H. Sugiyama, F. Otsuka, Y. Sato, H. Makino, Vasohibin-1 deficiency enhances renal fibrosis and inflammation after unilateral ureteral obstruction, Physiol. Rep. 2 (2014).

[17] H. Kimura, H. Miyashita, Y. Suzuki, M. Kobayashi, K. Watanabe, H. Sonoda, H. Ohta, T. Fujiwara, T. Shimosegawa, Y. Sato, Distinctive localization and opposed roles of vasohibin-1 and vasohibin-2 in the regulation of angiogenesis, Blood 113 (2009) 4810–4818.

[18] M. Arias, S. Sauer-Lehnen, J. Treptau, N. Janoschek, I. Theuerkauf, R. Buettner, A.M. Gressner, R. Weiskirchen, Adenoviral expression of a transforming growth factor-beta1 antisense mRNA is effective in preventing liver fibrosis in bile-duct ligated rats, BMC Gastroenterol. 3 (2003) 29.